

**PREPARATION AND CHARACTERIZATION OF SUPPORTED GOLD
NANOPARTICLES AND THEIR CATALYTIC STUDIES IN THE
REDUCTION OF *p*-NITROPHENOL**

by

HANANI BINTI YAZID

**Thesis submitted in fulfillment of the requirements for the degree of Master of
Science**

MAY 2010

ACKNOWLEDGEMENT

I would like to express my deepest gratitude to my supervisors, Assoc. Prof. Dr. Rohana Adnan and Assoc. Prof. Dr. Shafida Abd. Hamid (UIA, Pahang) for their tremendous guidance, supervision, and encouragement throughout my research works. My gratitude also goes to Dr. Akhyar Farrukh for valuable discussions and assistance.

Special thanks to all the staffs from School of Chemical Sciences, especially to Mr. Chow, Mr. Clement, Mr. Megat and Mr. Ariffin. My gratitude also goes to Mr. Muthu, Mr. Johari, Ms. Jamilah and Mrs. Faizah from Electron Microscopy Unit, School of Biology, Mr. Hilman from Center of Drug Research (CDR) and Mr. Hazhar from School of Physics. The assistance from the staffs of Doping Control Centre (DCC), Mrs. Norhayati and Mr. Azman for GC-MS/MS analysis is appreciated.

Deepest gratitude to my friends from the organic group: Dr. Yasodha, Ms. Nornaemah, Mrs. Afsheen, Mrs. Noviany, Mr. Daniel Tan; nanoscience group: Ms. Norhashila, Ms. Suriani, Ms. Yeo Siew Yen, Ms. Noorul Ain, Ms. Tan Wei Leng, Ms. Rosniza, Dr. Noor Hana Haniff as well as to Ms. Affaizza, Ms. Rozaini, Mr. Anwar, Mrs. Norhidaya, Ms. Sh. Zati Hanani, Ms. Ariza and Ms. Marina.

Heartfelt appreciation to my dearest family members: Mrs. Sharifah Bee, Mr. Hafizi, Mr. Hafizal and Ms. Haniza for their understanding, patience and moral support all the way till the completion of my research.

Last but not least, to Universiti Sains Malaysia (USM) for graduate assistant scheme (GA) and the financial support under FRGS grant-203/PKIMIA/671046 and PRGS grant-1001/PKIMIA/831002 are gratefully acknowledged.

TABLE OF CONTENTS

	Page numbers
Title	i
Acknowledgement	ii
Table of contents	iv
List of tables	viii
List of figures	x
List of scheme	xiv
List of abbreviations	xv
List of publication	xvii
Abstract	xviii
Abstrak	xx

CHAPTER 1: INTRODUCTION

1.1. Introduction	1
1.2. Problem statements	2
1.3. Research objectives	3
1.4. Scope of the research	3

CHAPTER 2: LITERATURE REVIEWS

2.1.	Nanomaterials and nanotechnology	5
2.2.	Current applications of nanotechnology	7
2.3.	Synthetic routes for the preparation of nanostructures	10
2.4.	Structural characterization	15
2.5.	Catalysts	16
2.5.1.	Unsupported and supported catalysts	17
2.5.2.	Noble metal catalysts	17
2.5.3.	Supports	19
2.6.	Gold catalyst	19
2.6.1.	Synthesis of supported gold nanoparticles	21
2.6.2.	Chemical reactions catalyzed by supported gold nanoparticles	23
2.7.	Reduction of <i>p</i> -nitrophenol	26
2.8.	Reaction kinetics	30

CHAPTER 3: MATERIALS AND METHODS

3.1.	Chemicals	32
3.2.	Sample notations	32
3.3.	Experimental method	33
3.3.1.	Preparation of metal oxide support	33
3.3.2.	Preparation of Au nanoparticles supported on metal oxides	33
3.3.3.	Catalytic activity	35
3.4.	Characterization techniques	36

CHAPTER 4: RESULTS AND DISCUSSION

4.1.	Metal oxides supported Au nanoparticles prepared by deposition-precipitation (DP) method	39
4.2.	Morphological features of Au/TiO ₂	42
4.2.1.	Titania	42
4.2.2.	Effect of pH below and above the isoelectric point (IEP) of titania for Au/TiO ₂	45
4.2.3.	Effect of pH adjustment	53
4.3.	Morphological features of Au/ZnO	59
4.3.1.	Zinc(II) oxide	59
4.3.2.	Effect of pH below and above the isoelectric point (IEP) of zinc(II) oxide for Au/ZnO	63
4.3.3.	Effect of pH adjustment	70
4.4.	Morphological features of Au/Al ₂ O ₃	75
4.4.1.	Alumina	75
4.4.2.	Effect of pH below and above the isoelectric point (IEP) of alumina for Au/Al ₂ O ₃	77
4.4.3.	Effect of pH adjustment	84
4.4.4.	Grafting of Au complexes	90
4.5.	Effect of metal oxide supports on the physicochemical properties of Au particles	94
4.5.1.	Physicochemical properties of Au	94
4.5.2.	Modes of attachment between Au and the supports	97

4.6.	Catalytic activity of <i>p</i> -nitrophenol	99
4.6.1.	Introduction	99
4.6.2.	Au/TiO ₂ series	100
4.6.3.	Au/ZnO series	102
4.6.4.	Au/Al ₂ O ₃ series	104
4.6.5.	Comparisons of <i>k</i> values with the literatures in the Au catalytic system	106
4.6.6.	Reusability and recharacterization of supported Au nanoparticles	107
CHAPTER 5: CONCLUSIONS		
5.1.	Conclusions	110
5.2.	Recommendations for future research	112
REFERENCES		113
APPENDICES		129

LIST OF TABLES

Table 2.1	The characterization techniques for nanomaterials	16
Table 2.2	The rate laws of zero order, first order and second order reactions	31
Table 3.1	Sample notations and the description	33
Table 4.1	The Au particle size, interparticle distance, loadings and surface area of the Au/TiO ₂ prepared at pH 5 and 7	50
Table 4.2	The pHs of gold chloride solutions at three intervals for Au/TiO ₂	54
Table 4.3	The physical properties of Au, loadings and surface area for Au/TiO ₂	57
Table 4.4	The Au particle size, interparticle distance, loadings and surface area of the Au/ZnO at pH 7 and pH 11	69
Table 4.5	The pHs of gold chloride solutions at three intervals for Au/ZnO	70
Table 4.6	The physical properties of Au, loadings and surface area for Au/ZnO	74
Table 4.7	The Au particle size, interparticle distance, loadings and surface area of the Au/Al ₂ O ₃ at pH 5 and 11	84
Table 4.8	The pH of gold chloride solutions at three intervals for Au/Al ₂ O ₃	85
Table 4.9	The physical properties of Au, loadings and surface area for Au/Al ₂ O ₃	89
Table 4.10	The Au particle size and loadings, surface area and <i>k</i> values for TiO ₂ and Au/TiO ₂ series	101
Table 4.11	The Au particle size and loadings, surface area and <i>k</i> values for ZnO and Au/ZnO series	102
Table 4.12	The Au particle size and loadings, surface area and <i>k</i> values for Al ₂ O ₃ and Au/Al ₂ O ₃ series	104

Table 4.13	Comparisons of the rate constant for the reduction of <i>p</i> -nitrophenol over Au catalysts in several different systems	107
Table 4.14	The <i>k</i> values of supported Au nanoparticles for each cycles in the reusability tests	107

LIST OF FIGURES

Figure 2.1	Sequence of events during spray pyrolysis process	11
Figure 2.2	SEM images of (a) ZnO nanorods on Al ₂ O ₃ substrate by PVD method [33] and (b) carbon nanotubes on Ni polycrystalline substrate by CVD method [34]	12
Figure 2.3	(a) Normal micelle and (b) reverse micelle	13
Figure 2.4	The chemisorption energies of several transition metals in eV [80]	20
Figure 2.5	Transformation of 4-nitrophenol to 4-nitrosophenol, 4-hydroxylaminophenol and 4-aminophenol in the presence of NADH [140]	28
Figure 3.1	Process of the preparation of Au nanoparticles supported on metal oxides by deposition-precipitation method	35
Figure 4.1	The dependence of the concentrations of gold precursors species derived from [AuCl ₄] ⁻ by hydrolysis on pH, total [Au] = 4x10 ⁻³ M [151]	40
Figure 4.2	UV-Vis spectra for gold solution at 80 °C for pH (a) 1.75, (b) 5.00 and (c) 6.50	41
Figure 4.3	DR UV-Vis spectrum for the commercial TiO ₂	43
Figure 4.4	XRD diffractogram for titania (anatase) at 2θ: 30° to 120° and its crystal lattices	43
Figure 4.5	SEM image for the commercial titania [Scale bar: 1 μm]. The inserted image shows the elemental composition of titania by EDX analysis	44
Figure 4.6	TEM images of titania viewed at low and high magnifications [Scale bar 200 nm]	44
Figure 4.7	The appearance of Au/TiO ₂ for (a) DP2 C7 and (b) DP2 C5	45
Figure 4.8	DR UV-Vis spectra of Au/TiO ₂ for (a) below the IEP of titania: DP2 C5 and (b) above the IEP of titania: DP2 C7	46
Figure 4.9	XRD diffractograms of Au/TiO ₂ for (a) below the IEP of titania: DP2 C5 and (b) above the IEP of titania: DP2 C7	48

Figure 4.10	TEM micrographs of Au/TiO ₂ for (a) below the IEP of titania: DP2 C5 and (b) above the IEP of titania: DP2 C7 [Scale bar: 50 nm]. The inserted images are the Au particle size distributions	49
Figure 4.11	SEM images of Au/TiO ₂ for (a) below the IEP of titania: DP2 C5 and (b) above the IEP of titania: DP2 C7 [Scale bar: 100 nm]. The inserted images are the spectra of the EDX analysis	51
Figure 4.12	The appearance of Au/TiO ₂ for (a) one-time pH adjustment: DP1 C7 and (b) without pH adjustment: DP0	53
Figure 4.13	XRD diffractograms of Au/TiO ₂ for (a) one-time pH adjustment: DP1 C7 and (b) without pH adjustment: DP0	55
Figure 4.14	TEM micrographs of Au/TiO ₂ for (a) one-time pH adjustment: DP1 C7 with the inserted image of particles size distribution and (b) without pH adjustment: DP0 [Scale bar: 50 nm]	56
Figure 4.15	FT-IR spectra of the prepared ZnO (a) before and (b) after calcination at 450 °C compared with insert image of FT-IR spectra for ZnO (a) before and (b) after calcination by Souza <i>et al.</i> [149]	60
Figure 4.16	XRD diffractograms for ZnO at 2θ: 30° to 70° (a) before calcination and (b) after calcination with its crystal planes	61
Figure 4.17	SEM image for the prepared ZnO after calcination at 450 °C with the inserted image of the elemental composition of ZnO by EDX analysis [Scale bar: 1 μm]	62
Figure 4.18	TEM image of the prepared ZnO after calcination at 450 °C	62
Figure 4.19	The appearance of Au/ZnO for (a) DP2 C7 and (b) DP2 C11	63
Figure 4.20	DR UV-Vis spectra of Au/ZnO for (a) below the IEP of zinc oxide: DP2 C7 and (b) above the IEP of zinc oxide: DP2 C11	64
Figure 4.21	XRD diffractograms of Au/ZnO for (a) below the IEP of zinc oxide: DP2 C7 and (b) above the IEP of zinc oxide: DP2 C11	65

Figure 4.22	TEM micrographs of Au/ZnO for (a) below the IEP of zinc oxide: DP2 C7 with the inserted image of Au particle size distribution and (b) above the IEP of zinc oxide: DP2 C11 [Scale bar: 50 nm]	66
Figure 4.23	SEM images of Au/ZnO for (a) below the IEP of zinc oxide: DP2 C7 [Scale bar: 2 μ m] and (b) above the IEP of zinc oxide: DP2 C11 [Scale bar: 200 nm] with the inserted images of EDX spectra	68
Figure 4.24	The appearance of Au/ZnO for (a) one-time pH adjustment: DP1 C7 and (b) without pH adjustment: DP0	70
Figure 4.25	XRD diffractograms of Au/ZnO for (a) one-time pH adjustment: DP1 C7 and (b) without pH adjustment: DP0	72
Figure 4.26	TEM micrographs of Au/ZnO for (a) one-time pH adjustment: DP1 C7 and (b) without pH adjustment: DP0 [Scale bar: 50 nm]. The inserted image is the Au particle size distribution chart	73
Figure 4.27	XRD diffraction pattern for the commercial Al ₂ O ₃ used and its crystal lattices	75
Figure 4.28	TEM image of the commercial alumina at high magnification	76
Figure 4.29	SEM image of the commercial Al ₂ O ₃ used with the inserted graph of the elemental composition of Al ₂ O ₃ by EDX analysis	77
Figure 4.30	The appearance of Au/Al ₂ O ₃ for (a) DP2 C5 and (b) DP2 C11	78
Figure 4.31	DR UV-Vis spectra of Au/Al ₂ O ₃ for (a) above the IEP of alumina: DP2 C11 and (b) below the IEP of alumina: DP2 C5	79
Figure 4.32	XRD diffractograms of Au/Al ₂ O ₃ for (a) below the IEP of alumina: DP2 C5 and (b) above the IEP of alumina: DP2 C11	80
Figure 4.33	TEM micrographs of Au/Al ₂ O ₃ for (a) below the IEP of alumina: DP2 C5 with the inserted graph of Au particle size distribution chart and (b) above the IEP of alumina: DP2 C11 [Scale bar: 50 nm]	81

Figure 4.34	SEM image of Au/Al ₂ O ₃ at 10 k magnification for (a) below the IEP of alumina: DP2 C5 and (b) DP2 C11 [Scale bar: 1 μm] with the inserted images of the EDX spectra	83
Figure 4.35	The appearance of Au/Al ₂ O ₃ for (a) two-time pH adjustments: DP2 C7, (b) one-time pH adjustment: DP1 C7 and (c) without pH adjustment: DP0	85
Figure 4.36	The DR UV-Vis spectra of Au/Al ₂ O ₃ for (a) without pH adjustment: DP0, (b) one-time pH adjustment: DP1 C7 and (c) two-time pH adjustments: DP2 C7	86
Figure 4.37	XRD diffractograms of Au/Al ₂ O ₃ for (a) two-time pH adjustments: DP2 C7, (b) one-time pH adjustment: DP1 C7 and (c) without pH adjustment: DP0	87
Figure 4.38	TEM micrographs of Au/Al ₂ O ₃ for (a) DP2 C7 [Scale bar: 20 nm], (b) DP1 C7 [Scale bar: 50 nm] and (c) DP0 [Scale bar: 20 nm]. The inserted images are the Au particle size distribution charts	89
Figure 4.39	Formation of surface species on alumina [171]	91
Figure 4.40	The possible colours of Au nanoparticles supported on magnesia, alumina and silica [165]	94
Figure 4.41	The possible modes of attachment of the Au precursors on the support for Au/TiO ₂ , Au/ZnO and Au/Al ₂ O ₃ systems	98
Figure 4.42	Plots of ln (A _t -A _∞) versus time for the reduction of <i>p</i> -NP with Au/TiO ₂ catalysts	102
Figure 4.43	Plots of ln (A _t -A _∞) versus time for the reduction of <i>p</i> -NP with Au/ZnO catalysts	103
Figure 4.44	Plots of ln (A _t -A _∞) versus time for the reduction of <i>p</i> -NP with Au/Al ₂ O ₃ catalysts	105
Figure 4.45	TEM images and reusability charts of (a) DP2 C7 Au/TiO ₂ , (b) DP2 C7 Au/ZnO and (c) DP2 C11 Au/Al ₂ O ₃	108

LIST OF SCHEME

Scheme 1	Formation of <i>p</i> -nitrophenolate ion in alkaline condition	100
----------	---	-----

LIST OF ABBREVIATIONS

AAS	Atomic absorption spectroscopy
AFM	Atomic force microscopy
Au/SiO ₂	Silica supported Au nanoparticles
Au@SiO ₂	Au particles coated by silica (yolk/shell structure)
BET	Brunauer, Emmett and Teller
CNT	Carbon nanotube
CVD	Chemical vapour deposition
DP	Deposition-precipitation
DP NaOH	Deposition-precipitation by sodium hydroxide
DP Urea	Deposition-precipitation by urea
DP0	Deposition-precipitation without pH adjustment
DP1	Deposition-precipitation with one-time pH adjustment
DP2	Deposition-precipitation with two-time pH adjustment
DR UV-Vis	Diffuse reflectance ultraviolet-visible spectroscopy
EDX	Energy dispersive X-ray detection
FGME	Full-grown metal nanoparticles
FT-IR	Fourier transform-infrared
ICDD	International Centre Diffraction Data
IEP	Isoelectric point
K	Kelvin (temperature unit)
MO _x	Metal oxide
NAD	Nicotinamide adenine dinucleotide

NADH	Nicotinamide adenine dinucleotide-hydrogen
PAMAM	Poly(amidoamine)
PMMA	Poly(methyl methacrylate)
PPI	Poly(propyleneimine)
PVA	Polyvinylalcohol
PVD	Physical vapour deposition
PVP	Polyvinylpyrrolidone
rt	Room temperature
SEM	Scanning electron microscopy
SMSI	Strong metal support interaction
SPR	Surface plasmon resonance
TEM	Transmission electron microscopy
TPPTS	Trisodiumtris(<i>m</i> -sulfonatophenyl)phosphine) ₂
UA	Unsaturated alcohol
XRD	Powder X-ray diffraction
WGS	Water-gas shift
pH _i	Initial pH
pH _t	pH after the addition of support to the gold precursor solution
pH _f	Final pH after all adjustment
fcc	Face-centered cubic
<i>p</i> -NP	<i>p</i> -nitrophenol
λ _{max}	Wavelength of maximum absorbance (nm)

LIST OF PUBLICATIONS

1. H. Yazid, R. Adnan, S. A. Hamid, M. A. Farrukh, "Synthesis of gold nanoparticles supported on zinc oxide via deposition precipitation method", *Turk. J. Chem.* **34** (2010) 639-650.
2. H. Yazid, R. Adnan, S. A. Hamid, M. A. Farrukh, "Synthesis of gold nanoparticles supported on titania: active catalyst for the reduction of 4-nitrophenol using hydrazine", *J. Iran. Chem. Soc.*, 2010 - *submitted*
3. H. Yazid, R. Adnan, S. A. Hamid, M. A. Farrukh, "Synthesis of Au/Al₂O₃ nanocatalyst and its application in the reduction of *p*-nitrophenol", *J. Chin. Chem. Soc.*, 2010 - *submitted*
4. H. Yazid, R. Adnan, S. A. Hamid, M. A. Farrukh, "Preparation and characterization of alumina supported gold nanoparticles and its application in the reduction of *p*-nitrophenol", 3rd Penang International Conference of Young Chemists (ICYC 2010), Penang, 23-25 June 2010.
5. H. Yazid, R. Adnan, S. A. Hamid, "Synthesis and characterization of gold nanoparticles supported on metal oxide by deposition-precipitation method" Research Colloquium of School Chemical Sciences 2009, Penang, 2-3 November 2009.
6. H. Yazid, R. Adnan, S. A. Hamid, "Preparation and characterization of gold catalyst supported on alumina by deposition-precipitation method" 13th Asian Chemical Congress (13 ACC 2009), Shanghai, 13-16 September 2009.
7. H. Yazid, S. A. Hamid, R. Adnan, "Synthesis of Supported Gold Nanocatalyst: Characterization and Application in Hydrogenation Reaction" ChemBio Tech '08 (A Regional Conference on Chemical & Biomolecular Engineering), Singapore, 19-20 December 2008.
8. H. Yazid, S. A. Hamid, R. Adnan, "Synthesis of Au/TiO₂ and Its Application in Hydrogenation of Citral" 2nd Penang International Conference of Young Chemists (ICYC 2008), Penang, 18-20 June 2008.

**PREPARATION AND CHARACTERIZATION OF SUPPORTED GOLD
NANOPARTICLES AND THEIR CATALYTIC STUDIES IN THE
REDUCTION OF *p*-NITROPHENOL**

ABSTRACT

Gold (Au) nanoparticles supported on titania (TiO₂), alumina (Al₂O₃) and zinc oxide (ZnO) were prepared by the deposition-precipitation (DP) method using gold (III) chloride trihydrate, HAuCl₄·3H₂O as the precursor. The effect of pH on Au loadings, particle size and particle size distribution in the preparation of the gold nanoparticles were studied at pH below and above the isoelectric points (IEP) of the metal oxide supports. The effects of adjusting pH before and after the addition of the support into the gold precursor solution were also investigated. Structural and elemental characterizations of the supported gold nanoparticles were carried out using X-ray diffraction (XRD), transmission electron microscopy (TEM), scanning electron microscopy (SEM), energy-dispersive X-rays (EDX), atomic absorption spectrometry (AAS), ultraviolet-visible spectroscopy (UV-Vis) and Brunauer, Emmett and Teller (BET) adsorption method. The results revealed the dependency of Au particles size on the gold precursor species present at the pH of the preparation. The Au particle size obtained range between 4 - 8 nm. The Au/ZnO system produced the smallest Au particles size (4.32 ± 1.26 nm). The effect of pH adjustment furthermore emphasized the crucial of pH_t (pH after the addition of support to the gold precursor solution) in determining the types of gold complexes deposited on the support. The final pH (pH_f) showed a more pronounced effect in terms of the total Au loadings in the sample. The

catalytic activities of the prepared supported Au nanoparticles were tested in the reduction of *p*-nitrophenol (*p*-NP) in the presence of hydrazine as a reductant. The catalytic reaction was monitored spectrophotometrically based on pseudo first order kinetic model. All the Au/MO_x systems (Au/TiO₂, Au/ZnO, Au/Al₂O₃) exhibited the best catalytic activity produced by DP method with two-time pH adjustments. The comparisons on the rates constants (*k*) showed the highest catalytic activity was achieved in Au/MO_x system with smaller Au particle size (4.45 ± 1.80 nm), higher surface area ($23.47 \text{ m}^2 \text{ g}^{-1}$) and higher Au loadings (2.653 %) in the order of ZnO > TiO₂ > Al₂O₃. The Au/ZnO showed the highest *k* value of $20.5 \times 10^{-3} \text{ s}^{-1}$ followed by Au/TiO₂ ($16.9 \times 10^{-3} \text{ s}^{-1}$) while Au/Al₂O₃ was the least active ($12.7 \times 10^{-3} \text{ s}^{-1}$). The least activity shown by Au/Al₂O₃ was attributed to the presence of cationic Au as the more dominant species in the sample. All the catalysts can be reused without causing a significant change in the rate constants even after 3 cycles. The leaching of Au nanoparticles into the reaction solution also did not occur which reflect the stability of the prepared catalysts.

Keywords: Gold nanoparticles, deposition-precipitation method, *p*-nitrophenol, metal oxide

**PENYEDIAAN DAN PENCIRIAN NANOZARAH EMAS TERSOKONG DAN
KAJIAN PEMANGKINANNYA DALAM TINDAK BALAS PENURUNAN *p*-
NITROFENOL**

ABSTRAK

Nanozarah emas tersokong titanium oksida, aluminium oksida and zink oksida telah disediakan berdasarkan kaedah pengenaan-pemendakan dengan menggunakan aurum (III) klorida trihidrat, $\text{HAuCl}_4 \cdot 3\text{H}_2\text{O}$ sebagai bahan pemula. Kesan pH terhadap kuantiti, saiz dan taburan saiz partikel dalam penyediaan nanozarah emas telah dikaji pada pH di bawah dan di atas titik isoelektrik (IEP) bagi oksida logam. Kajian turut dilakukan terhadap kesan pelarasan pH sebelum dan selepas penambahan penyokong ke dalam larutan bahan pemula. Pencirian struktur dan elemen nanozarah emas tersokong dilakukan melalui kaedah pembelauan sinar-X (XRD), mikroskop elektron transmisi (TEM), mikroskop elektron pengimbasan (SEM), penyebaran elektron sinar-X (EDX), spektroskopi penyerapan atom (AAS), spektroskopi ultraungu-nampak (UV-Vis) dan kaedah penjerapan Brunauer, Emmett and Teller (BET). Keputusan menunjukkan kebergantungan saiz terhadap spesies bahan pemula emas yang hadir pada pH penyediaan. Julat bagi saiz partikel emas yang diperolehi adalah di antara 4 - 8 nm. Sistem Au/ZnO menghasilkan saiz partikel emas terkecil (4.32 ± 1.26 nm). Kesan dari pelarasan pH selanjutnya menunjukkan pengaruh pH_t (pH selepas kemasukan penyokong ke dalam larutan bahan pemula) dalam menentukan jenis kompleks emas yang terbentuk di atas penyokong. pH akhir (pH_f) menunjukkan kesan yang jelas dari aspek muatan keseluruhan Au di dalam sampel. Aktiviti pemangkinan nanozarah emas

tersokong yang telah dihasilkan diuji dalam tindak balas penurunan *p*-nitrofenol (*p*-NP) dengan kehadiran hidrazin sebagai bahan penurun. Tindak balas bermangkin ini diukur secara spektrofotometri berdasarkan model kinetik tertib pseudo pertama. Kesemua sistem Au/MO_x (Au/TiO₂, Au/ZnO, Au/Al₂O₃) mempamerkan aktiviti pemangkinan tertinggi bagi kaedah DP dengan 2 kali pelarasan pH. Perbandingan bagi pemalar kadar (*k*) menunjukkan aktiviti pemangkinan tertinggi dicapai dalam sistem Au/MO_x dengan partikel Au bersaiz kecil (4.45 ± 1.80 nm), luas permukaan ($23.47 \text{ m}^2 \text{ g}^{-1}$) dan muatan Au (2.653 %) yang tinggi mengikut urutan ZnO > TiO₂ > Al₂O₃. Au/ZnO menunjukkan nilai *k* tertinggi iaitu $20.5 \times 10^{-3} \text{ s}^{-1}$ diikuti oleh Au/TiO₂ ($16.9 \times 10^{-3} \text{ s}^{-1}$) dan Au/Al₂O₃ adalah yang paling kurang aktif ($12.7 \times 10^{-3} \text{ s}^{-1}$). Keaktifan terendah ditunjukkan oleh Au/Al₂O₃ adalah disebabkan kehadiran kationik Au sebagai spesies yang lebih dominan di dalam sampel. Kesemua mangkin boleh digunakan semula tanpa menyebabkan perubahan ketara terhadap pemalar kadar tindak balas walaupun selepas 3 kali kitaran. Larut-lesap nanozarah emas ke dalam larutan tindak balas juga tidak berlaku dan ini menunjukkan kestabilan mangkin yang telah disediakan.

Kata kunci: Nanozarah emas, kaedah penganapan-pemendakan, *p*-nitrofenol, oksida logam

CHAPTER 1

INTRODUCTION

1.1. Introduction

Achieving nano-size materials in a particular size range is one of the great scientific interests due to the fact that the properties of materials can be very different from those at a larger scale [1]. Gold (Au) particularly is one of the best examples to illustrate the change of properties of material when it is converted to nanosize. Gold was considered to be an inert, chemically uninteresting metal and the least catalytically useful [2, 3]. This fact changed in the 1980s when small gold particles supported on metal oxides was successfully prepared and proved to be active in the oxidation of carbon monoxide at low temperatures [4]. This breakthrough focused the attention on gold's property and drastically changes the position of gold in catalysis. Catalysis by gold is preferred rather than classical metal catalyst due to its selectivity in particular reactions under mild conditions [3].

Some of the earliest utilizations of supported gold catalyst were oxidation reaction of carbon monoxide and epoxidation of propylene. This promising start was then followed by hydrogenation reaction of α , β -unsaturated aldehydes and ketones. Recently the gold catalysts were reported to be selective in reducing nitro into amino groups with the presence of other easily reducible groups such as double bond and carbonyls. This unique selectivity of gold catalytic activity makes it an interesting field to explore and deserves to be deeply investigated.

1.2. Problem statements

Small Au particles of 3 - 5 nm size range is favourable in order to catalyze many organic reactions [5]. However, achieving the nano size particles can be challenging since many factors can affect the size of the Au particle. One of the crucial factors is the preparation method [3]. The selection of suitable preparation method is necessary in order to obtain the desired Au features. In this work, the preparation of the Au nanoparticles is by deposition-precipitation (DP) method. This method is always associated with the production of highly active supported gold nanoparticles [6-8]. The pH of the preparation in DP method is mainly focused and other parameters such as Au concentration, reaction temperature and calcination procedure are maintained throughout the experiment.

The reduction reaction of *p*-nitrophenol is chosen to test the prepared supported Au nanoparticles activity. *p*-nitrophenol is a common organic pollutant which causes harmful effect to biological systems due to its toxicity, and now is of great public concern. Many methods have been developed to remove the hazardous *p*-nitrophenol in industrial and agricultural waste water including catalytic reduction. In fact the reduction of *p*-nitrophenol produces *p*-aminophenol, which is an important intermediate for the manufacture of analgesic and antipyretic drugs. Besides that there is also a great demand of the aromatic amino compounds in industry. Therefore this reaction becomes important academically as well as industrially and opens up the opportunities to the development of methodologies for catalyzing organic reactions in aqueous solutions [9].

1.3. Research objectives

The objectives of the research were:

- (a) To synthesize and characterize active gold nanoparticles supported on titania (Au/TiO₂), alumina (Au/Al₂O₃) and zinc oxide (Au/ZnO).
- (b) To study the effect of pH below and above the isoelectric point (IEP) of the metal oxide supports as well as the effect of adjusting the pH before and after the addition of the support into the gold precursor solution on Au particle size, particles distribution and Au loadings.
- (c) To study the catalytic activity of the Au/TiO₂, Au/ZnO and Au/Al₂O₃ in the reduction reaction of *p*-nitrophenol in the presence of hydrazine which acts as a reductant.

1.4. Scope of the thesis

The scope of the thesis consists of 5 parts. It starts with a brief introduction to the research topic in Chapter 1, followed by the literature review in Chapter 2. Chapter 3 presents the reagents used and the experimental procedures. The results and discussion are included in Chapter 4. Here we discussed the preparation of the supported Au nanoparticles by the deposition-precipitation method, the properties of the metal oxide supports used, together with the effect of pH below and above the IEP of metal oxides as well as the effect of pH adjustment on Au/TiO₂, Au/ZnO and Au/Al₂O₃ systems. The effect of each support on the physicochemical properties of Au and the possible types of Au attachment on the supports were also discussed. The catalytic activity of the prepared Au nanoparticles in reduction reaction of *p*-nitrophenol is

explained in Section 4.6. Lastly, the findings of this research work are concluded in Chapter 5 followed by some recommendations for future work.

CHAPTER 2

LITERATURE REVIEWS

2.1. Nanomaterials and nanotechnology

Nanoscience is a study of phenomena and manipulations of materials at atomic, molecular and macromolecular scales in which the properties of materials differ significantly from those at larger scale. The prefix ‘nano’ originated from the Greek word for ‘dwarf’. Any matter with one of its dimensions whether width, length or height is in nanometer scale is defined as nanomaterial. Nanomaterials constitute the use of devices with smaller dimensions for which a new physical behaviour naturally emerges. Scientifically 1 nm is equal to 10^{-9} m. These nanomaterials can be metals, clays, polymers, semiconductors, etc. Several terms which are associated as well as explain nanomaterials are presented as the following [10, 11]:

- (i) Cluster: A group of two or more metals atoms bound by metal-metal bonds.
- (ii) Colloid: A system which has two or more dispersed and continuous phases. The dispersed phase distributes in the continuous phase, and one of these phases has dimensions of 10^{-9} to 10^{-6} m range. In particular, colloid can be classified in various ways such as sol, emulsion and gel.

Sol is the dispersion of small solid particles in a liquid. The particles can be macromolecules or a cluster of small molecules. Emulsion is a colloidal system in which the dispersed and continuous phases are both liquids such as oil in water. Meanwhile gel is a colloidal system in which both the dispersed and

continuous phases have a three dimensional network throughout the material, in the form of jelly-like mass.

- (iii) Crystal: A solid with a regular polyhedral shape.
- (iv) Crystalline: Materials having internal arrangement of atoms in a regular pattern repetition in three dimensions.
- (v) Nanoparticles: Ultrafine particles with size between 1 to 100 nanometers.
- (vi) Nanocrystal: A solid particle of single crystal in the nanometer size range.
- (vii) Nanostructure: A material assembled from a layer or cluster of atoms with the size in the order of nanometers.
- (viii) Quantum dots: Semiconductors with conducting characteristics that are closely related to the size and shape of the individual crystal.

The term nanotechnology was coined by Norio Taniguchi and can be defined as the design, characterization, production and application of structures, devices and systems by controlling shape and size at the nano scale (The Royal Society and The Royal Academy of Engineering, 2004) [12]. Achieving nanosize materials are of tremendous importance for at least two specific reasons, which are (1) surface area and (2) quantum size effects.

1. Surface area: An increment of surface area compared to the same mass of material produced in the larger amount makes the materials reactive and affects the change in their strength and electrical properties.

2. Quantum size effects: Quantum size effects begin to dominate the behaviour of matter at the nanoscale, and affects the optical, electrical and magnetic properties of materials.

2.2. Current applications of nanotechnology

The development of nanotechnology allows the production of a large set of improved materials with weight reduction and enhancement in its stability and functionality. Some of the current applications of nanotechnology in several different fields are categorized as follows:

- (i) Electronic and magnetic

The demand of an improved information storage in terms of its capacity and bandwidth for conventional hard disks, probe-based and patterned media magnetic recording keeps increasing. With the approach of nanotechnology, this demand becomes viable in achieving areal densities of 1 Terabyte inch⁻². Juang and Bogy fabricated self-assembled nanoporous alumina templates for the patterned media by an adequate selection of electrolytes, anodizing voltage and etching time. This nanoporous alumina exhibited an ultrahigh areal density with ordered structures [13]. Meanwhile recent advances in magnetic nanotechnology allow the fabrication of high quality magnetic nanoparticles with self-organized lattices. Luis *et al.* investigated the dipole-dipole interaction exerted on the dynamics of magnetization of nanometer-sized Co-clusters for better applications in high density recording media [14].

(ii) Biomedical

The integration of nanomaterials in biological and medical research produces sensors and biomarkers. Zare *et al.* introduced a simple colourimetric sensor for the detection of conformational change of protein by using gold nanoparticles [15]. Naturally every protein folds in a unique three-dimensional shape for it to function specifically. However under certain conditions, these proteins can change its shapes which medically signify any infection in the blood stream. A gold nanoparticle sensor has been developed to detect this sign by visualizing the changes of colour when folded or unfolded proteins are attached to it [15]. Recently gold nanoparticle has been used as a biomarker for the detection of Alzheimer disease [16]. This detection is based on the antibody-antigen interaction, in which the antibody-conjugated gold nanoparticle bind with tau protein (protein for Alzheimer disease detection) which further produces nanoparticle aggregation. This aggregation resulted in colourimetric change and a new band appeared around 150 nm, far from its usual plasmon absorption band at 530 nm.

(iii) Chemical reaction

Chemical reaction is a process of the transformation of one set of chemical substances into another. This reaction can be either spontaneous or requires energy such as heat, light or electricity. In most of the cases, a catalyst is used to accelerate the reaction and consequently obtains desired products. Nanoparticles catalysts are highly active since most of the particle surfaces can be available to catalysis. Generally, the size of the nanoparticles catalysts can be in the ranged of 2 – 85 nm for their applications in various catalytic reactions [17]. The applications include the production

of fine chemicals [18], fuel cell [19], catalytic converters [20, 21] and photocatalytic devices.

(iv) Environmental and green chemistry

Manufacturing causes pollution and pollution is a sign of poor technology developed and an inadequate control of how materials are handled. Alternative routes for avoiding this is by producing less waste and creating superior products with versatile and reproducible technique. Adsorbent is one of the environmental products which utilize the application nanotechnology. Metal oxides nanoparticles have high surface reactivities which enable them to chemisorb chemical species and toxic substances irreversibly [22]. The nanocrystalline Al_2O_3 , CaO , MgO [23] and ZnO have already been applied to adsorb acidic gases and polar organic compounds [24]. Besides, there are also metal nanotubes that are used as membrane filters. For example Wirtz and Martin synthesized Au nanotubes deposited on porous polymeric membranes by an electroless plating technique, particularly for the membrane-based chemical and biological separations [25].

(v) Consumer goods

Nanotechnology has also made an impact in the field of consumer goods by providing products with novel functions. For example in food packaging industry, a nanocomposite of anti-microbial agents are placed directly on the surface of the coated film to improve the traditional food packaging [26]. Nanocomposites can increase or decrease gas permeability of different fillers as needed for different products. Besides

that this package is more light resistance, has strong mechanical and thermal performance, which leads to an increase in the length of the shelf life [27]. Meanwhile the titanium oxide (TiO₂) nanoparticles are used as skin-protective compounds in sunscreens. Fine TiO₂ particles are embedded with sunscreens into the skin to efficiently attenuate harmful UV-B radiation coming from the sun [28].

2.3. Synthetic routes for the preparation of nanostructures

Generally there are two routes of synthesizing nanostructures which are ‘top-down’ and ‘bottom-down’ approaches [29]. The top-down approach starts from the bulk material and scales down to the nanosize, e.g. by mechanical grinding of the bulk materials. The drawback of this method is it is hardly suitable for the preparation of uniform and small size particles with less than 100 nm. Therefore this route is less favoured. The bottom-up approach is better in producing uniform particles with a specific size, shape and structure [30]. This approach involves the precipitation of a solid phase from a solution. The precipitation process basically consists of nucleation and growth stages [30]. Based on these nucleation steps, several methods of preparing nanoparticles have been anticipated and categorized as follows:

(i) Vapour phase synthesis: Spray pyrolysis, physical vapour deposition (PVD) and chemical vapour deposition (CVD) are listed in this category [30-33]. Spray pyrolysis relates to the atomization of metal precursor in solution which becomes fine droplets when spray into a thermal zone. In the thermal zone, the solvent evaporates and

reactions occur within each particle to form a product particle [31]. The sequence of events in spray pyrolysis process is shown in Figure 2.1.

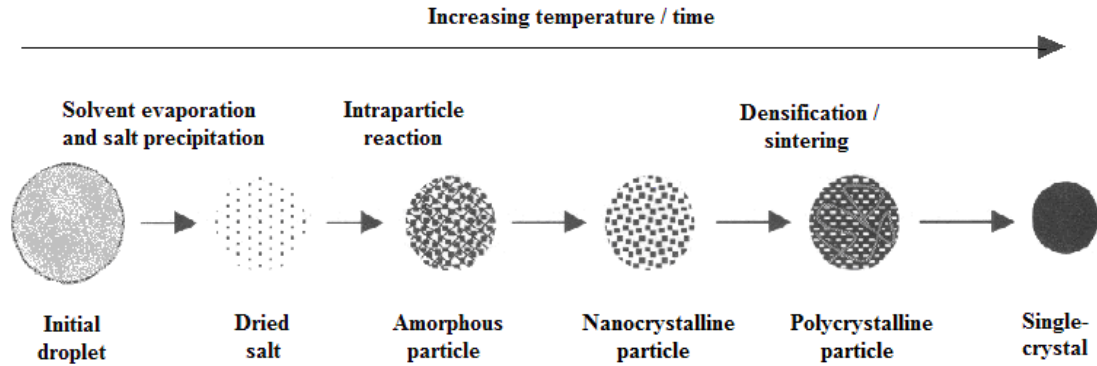


Figure 2.1: Sequence of events during spray pyrolysis process.

The PVD method consists of three main steps: (a) condensation of solid material into vapour phase by physical processes, (b) transporting the material to the substrate, and (c) formation of the particles by nucleation and growth [30]. Ordered nanostructures can be produced by controlling these three steps. It has been proven by Gao *et al.* that a well-aligned ZnO nanorods on a polycrystalline Al₂O₃ can be obtained by controlling the particle growth at a high deposition temperature (Figure 2.2a) [33]. The CVD method on the other hand engages with thermal decomposition of gas phase species at elevated temperatures, followed by subsequent deposition onto a substrate [32]. Carbon nanotube (CNT) is one of nanostructures that can be synthesised by this method. A variation in size and length of the carbon nanotubes can be achieved by altering the reaction conditions in the CVD method (Figure 2.2b) [34].

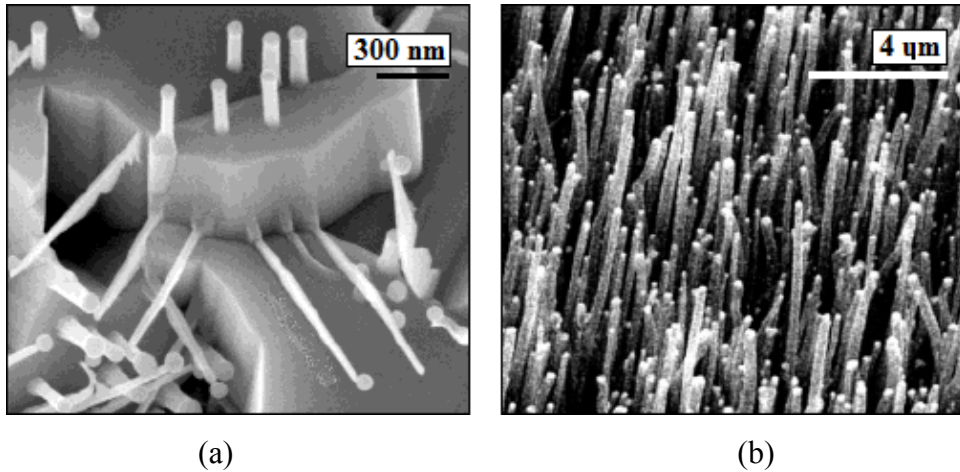


Figure 2.2: SEM images of (a) ZnO nanorods on Al₂O₃ substrate by PVD method [33] and (b) carbon nanotubes on Ni polycrystalline substrate by CVD method [34].

(ii) Solution processing synthesis: Solution processing synthesis is a broad category which consists of chemical precipitation, sol-gel, microemulsion and hydrothermal processes [30]. The chemical precipitation concerns the reduction of metals from solutions or suspensions of their salt precursors by a suitable reducing agent.

The sol-gel process is one of the most popular methods to prepare metal oxide nanoparticles [35-37]. This method can be divided into four steps: hydrolysis, polycondensation, drying and thermal decomposition. Initially the metal alkoxide precursor is dissolved in a solvent, followed by an addition of water, alcohol, acid or base for hydrolysis and condensation to occur. After the solution is condensed into gel, the solvent is removed by drying. Then, the sample was subjected to thermal decomposition through calcination in order to decompose the organic precursors [30]. The properties of sol-gel prepared powders depend on a large extent on the reaction conditions such as concentration of solvents, temperature and pH. The size of the

particles can be tuned by optimal governing of these factors. This technique is widely used to prepare titania [35], silica [38] and tin (IV) oxide [39].

Microemulsion process is related to liquid mixtures of oil, water and surfactant which can form micelle. The surfactant is an organic compound which contains both hydrophobic (tail) and hydrophilic (head) groups. Therefore, it is soluble in both organic solvent and aqueous phase. Micelle consists of a normal and a reverse micelle. Oil droplet in water is an example of a normal micelle. The hydrophobic hydrocarbon chains of the surfactants are oriented toward the interior of the micelle, leaving the hydrophilic groups of the surfactants in contact with the surrounding aqueous medium [30]. The length of the surfactant hydrocarbon chain controls the size of the droplets. The normal micelle acts as a polymer that controls the size of the nanoparticles. The CdS and Cu nanoparticles are successfully produced by normal micelle [18, 19]. Meanwhile, the reverse micelle are formed in a nonaqueous medium in which the hydrophilic headgroups are directed toward the core of the micelles and the hydrophobic groups are directed outward [40]. Figure 2.3 illustrates the normal and the reverse micelle.

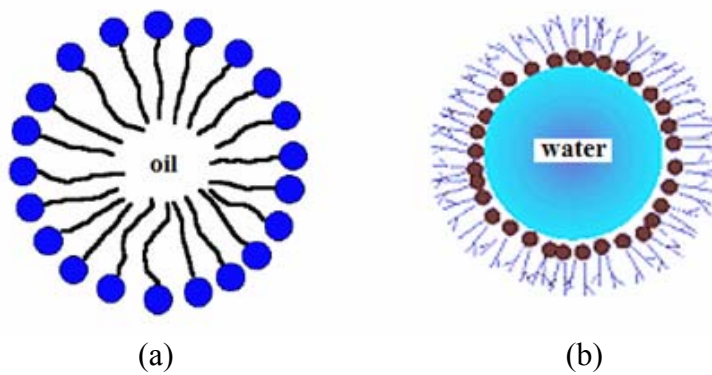


Figure 2.3: (a) Normal micelle and (b) reverse micelle.

Metal nanoparticles are synthesized by adding the reverse micelle solution containing reducing agent to the reverse micelle of the dissolved metal salt solution. The metal cations are then reduced to its metallic state. Certainly the reducing agent chosen must be stable in an aqueous environment and does not react with other components of the reverse micelle systems. The most common reducing agents used are sodium borohydride [41] and hydrazine [42].

The hydrothermal process utilizes the solubility of the inorganic substances in water at elevated temperatures and pressures. The subsequent crystallization of the dissolved material from the fluid generates the high quality of nanoparticles or nanocrystals. In order to achieve good distribution of nanocrystals, the control of water pressure, temperature, reaction time and the respective precursor-product parameters is necessary. Different types of BaTiO₃ [43], ZrO₂ [44] and PbS [45] have been successfully synthesized in this way.

(iii) Templated synthesis: Nanoparticles, nanotubes and nanorods of various materials can be synthesized by template-based approach [46]. This method consists of the fabrication of the desired material within the pores of channels of a nanoporous template. This approach is used to prepare nanometer-sized fibrils, rods, tubules of conducting polymers, metals and other solid matter [46]. Chemical polymerization [47], electrochemical [48] and electroless [49] depositions are grouped in this type of synthesis. The sol-gel deposition [50] and CVD [51] can also be categorized in this synthetic strategy.

2.4. Structural characterization

The spectroscopic and microscopic techniques such as infrared (IR) spectroscopy, ultraviolet-visible (UV-Vis) spectroscopy and atomic force microscopy (AFM) allow structural and elemental composition of nanomaterials to be obtained. The spectroscopic technique engages the study of interaction between radiation and matter as a function of either wavelength or frequency. Meanwhile the microscopic technique is a field which involves diffraction or reflection of electromagnetic radiation interacting with the subject of study to build up images. These techniques have become ‘the eye’ of nanomaterial since images are a very powerful means of presenting information. Brief descriptions of the characterization of the nanomaterials are presented in Table 2.1 as follows:

Table 2.1: The characterization techniques for nanomaterials.

Acronym	Full name and important highlights	Ref.
DR UV-Vis	Diffuse reflectance ultraviolet-visible spectroscopy <ul style="list-style-type: none"> ▪ Presents the surface plasmon resonance (SPR) band for metallic particle ▪ Presents degree of cluster aggregation 	[52, 53]
IR	Infrared spectroscopy <ul style="list-style-type: none"> ▪ Presents the information of the adsorbed species on the surface of materials 	[53]
AFM	Atomic force microscopy <ul style="list-style-type: none"> ▪ Real space imaging of material surface by monitoring the force exerted between the surface and the probe tip ▪ Not limited to conducting systems 	[54, 55]
SEM	Scanning electron microscopy <ul style="list-style-type: none"> ▪ Surface analysis ▪ Presents the information of the surface and subsurface microstructure of materials 	[56, 57]
TEM	Transmission electron microscopy <ul style="list-style-type: none"> ▪ Structural analysis ▪ Presents the information of the internal microstructure and defects of materials ▪ High resolution (HR): Produce images of atomic lattices 	[53]
XPS	X-ray photoelectron spectroscopy <ul style="list-style-type: none"> ▪ Surface analysis technique ▪ Identification of elemental composition, oxidation states and nearest neighbour bonding ▪ Elemental and chemical depth profile 	[58, 59]
XRD	Powder X-ray diffraction <ul style="list-style-type: none"> ▪ Identification of nanocrystalline phase ▪ Crystal size 	[11, 58]
EDX	Energy dispersive X-ray detection <ul style="list-style-type: none"> ▪ Performs qualitative or quantitative compositional analysis for elements 	[60]

2.5. Catalysts

Catalyst is a substance which facilitates chemical reactions without itself being consumed in the reaction. A catalyst works by changing the activation energy for a reaction to occur. This is accomplished by providing a new mechanism or reaction path through which the reaction can proceed. Catalysis is a term to describe the process of

changing the rate of a chemical reaction by catalyst. Basically there are two types of catalysis, homogeneous catalysis and heterogeneous catalysis. For homogeneous catalysis, the catalyst and the reactant occupy the same phase. This type of catalysis needs a relatively mild reaction condition and it is related to high selectivity and reproducibility. However the disadvantage of homogeneous catalysis lies in separating the catalyst and the product. In heterogeneous catalysis, the reactant and the catalyst are in different phases. The catalyst can be in unsupported or supported form.

2.5.1. Unsupported and supported catalysts

The unsupported catalyst can be composed of fixed (SiO_2 , zeolites) and variable (Ag_2O , V_2O_5) valence oxides, metal carbides or sulfides. Most of the active materials are not mechanically or thermally stable. Therefore the active component is deposited on a support for stabilization. The support material is usually chosen depending on the reactivity behaviour, high melting point and surface area. By using the support, an optimal dispersion of the active component and stabilization against sintering can be achieved.

2.5.2. Noble metal catalysts

Noble metal catalysts such as platinum (Pt), palladium (Pd) and silver (Ag) are among the common metal catalysts used to catalyze many organic reactions. These metals are usually synthesized as heterogeneous catalysts by depositing on supports such as carbon, metal oxides or polymers. For example Pt/C showed excellent activity in the liquid phase oxidation of cyclohexanol under a moderate temperature of 150 °C

and a pressure of 5 MPa using air as the oxidizing agent [61]. This reaction gave a total conversion of cyclohexanol of a 50 % selectivity to adipic acid, with glutaric and succinic acids as the main byproducts. Besides that, Pt supported on alumina showed good activity in the hydrogenation reaction of citral in cyclohexane and 2-pentanol [62].

The supported palladium catalysts were also tested in the hydrogenation of citral. The reaction yielded citronellal as the main product over PdCl₂(TPPTS), (TPPTS: trisodiumtris(*m*-sulfonatophenyl)phosphine)₂), [63] and Pd/Al₂O₃ [64]. The addition of additives: FeCl₂ for Pd on SiO₂/AlPO₄ system increased the selectivity towards geraniol and nerol in the same reaction [65]. Supported Pd catalysts are also active in the reduction of 4-nitrophenol with the highest catalytic activity was achieved for Pd on poly(propyleneimine) (PPI) dendrimers compared with Ag and Pt [66]. The reaction of Pd on poly-(3,4)ethylenedioxythiophene also exhibited good catalytic activity in this reaction [67].

In addition, the Ag nanoparticles were reported to catalyze the reduction of nitro compound. For example the *in situ* synthesized of Ag nanoparticles by Pradhan *et al.* were able to reduce aromatic nitro compounds to amines in an aqueous medium [68] while Liu *et al.* prepared Ag nanoparticles supported on halloysite nanotubes for the reduction of 4-nitrophenol [69].

Among the noble metals, gold is the least useful catalytically as it is inert towards most chemical reactions. However when fine gold particles are deposited on selected oxides, its chemistry drastically changes [4]. Gold showed a remarkable activity in selective oxidation [70] and reduction of particular organic reactions at low temperatures [71-73]. The details of the catalysis using gold will be explained in the following section.

2.5.3. Supports

The main supports used for depositing metal catalyst in the majority of the reported studies are activated carbon and metal oxides due to their inert property and a high surface area [74]. The metal oxides offer some variation in the property that can fall into the following categories: (i) supports that are active in reactions such as TiO₂, ZrO₂, ZnO, CeO₂, which act as the source of oxygen for the reaction and (ii) supports that are inert such as Al₂O₃, SiO₂ and MgO [75]. There are also some studies that group the metal oxides supports based on their reducible properties. The reducible supports such as TiO₂ or Nb₂O₅ exhibited a strong metal support interaction (SMSI) effect which can improve the selectivity of unsaturated alcohol in α , β -unsaturated aldehydes reaction [76, 77]. The types of supports used are also known to play an important role for the corresponding reaction [78].

2.6. Gold catalyst

Gold is one of the noble metals. The determination of the noble metal is measured by the ability of a metal surface to form bonds with a gas. In other words it is

illustrated by the ability of the metal surface to oxidize or to chemisorb oxygen dissociatively [79]. The calculated oxygen chemisorption energies on the face centered cubic (211) surface of several transition metals (except for Fe, Mo and W) are shown in Figure 2.4. From the figure, the transition metal above and to the left of Au in the periodic table show increasingly large chemisorption energy [80]. This indicates that these metals can bind weakly with oxygen. Au however has the endothermic chemisorption energy, which means it does not bind with oxygen at all. Therefore it is very unlikely that Au can be a good catalyst for an oxidation reaction. Surprisingly, gold was proven to be a very good catalyst for CO oxidation (typical reaction in an automotive exhaust system using Pt-based catalysts) at room temperature by Haruta and co-workers in 1980s [4, 81]. Since then, the synthesis of gold nanoparticles has aroused great scientific interest due to their various possible applications.

Cr	Mn	Fe - 6.30	Co -5.07	Ni -3.90	Cu -2.51
Mo -7.48	Tc	Ru -4.62	Rh -4.03	Pd -1.20	Ag -0.65
W -8.62	Re	Os	Ir -4.65	Pt -2.17	Au + 0.54

Figure 2.4: The chemisorption energies of several transition metals in eV [80].

Gold nanoparticles can be synthesized either by vacuum evaporation or by colloidal technique and are recognized as unsupported gold. Vacuum evaporation involves the deposition of thin films of metals on a substrate by evaporation in a

vacuum. Meanwhile, colloidal Au nanoparticles were prepared using various reducing agents which generated Au particles with sizes between 20 and 100 nm [82]. Unlike the colloidal technique, smaller particles with sizes less than 10 nm can be obtained by depositing gold onto a solid support. Gold catalysis activity is dependent on the size of Au particles and varied depending on the support [70, 83-85].

2.6.1. Synthesis of supported gold nanoparticles

Different methods for the synthesis of supported Au nanoparticles have been reported in the literature. Among these methods, the most quoted ones are impregnation, co-precipitation and deposition-precipitation [3].

(i) Impregnation was the earliest attempt of preparing supported Au nanoparticles. It is also considered as the simplest classical method. This method involves the addition of metal salt into a larger volume of the support suspension. The solution is then removed, followed by drying, calcination and reduction. The common support used in this method are silica [86], alumina [87, 88] and magnesia [89]. However, this method is less preferable as it tends to produce large gold particles [90].

(ii) Co-precipitation is commonly used to prepare supported base metal nanoparticles. The preparation engaged the addition of chloroauric acid solution and metal nitrate to a solution of sodium carbonate [91-93]. Two hydroxides formed and precipitated simultaneously in this step. Product particles were obtained after drying, calcination and reduction procedures. Highly dispersed gold nanoparticles on the

supports can be achieved by this method as reported on Au/ α -Fe₂O₃, Au/C₃O₄, Au/NiO and Au/Be(OH)₂, which are active for the low-temperature oxidation of carbon monoxide [81, 94].

(iii) Deposition-precipitation (DP) is the most frequently used procedure to synthesis gold nanoparticles. It can be applied to the widest range of support materials and are associated with small particle sizes with a uniform particle distribution as well as a closed interaction between the gold particles and the support [7, 95]. The name ‘deposition-precipitation’ was initially applied due to the assumption that the support would initiate the nucleation of Au(OH)₃. However, this is now seems differently. The metal oxide furthermore can be in the form of powder, bead, honeycomb or thin film. Raising the pH of the gold precursor solution can be done either by addition of base (usually NaOH: DP NaOH) or urea (DP Urea). The procedure using base required only 2 hours of aging time, while DP Urea needed about 16 hours due to its slow decomposition [96]. This decomposition slowed the precipitation of hydroxides which resulted in a more uniform Au particles [97].

Collectively, both DP methods have an advantage over other methods because the active component (gold chloride precursor) remains on the surface of the support and is not buried in it. Moreover, chloride ions which are known to poison the activity of gold nanoparticles in many types of reactions, can be minimized by repetitive washings [6]. Therefore, regardless of the numerous methods developed, DP still seems to be the most efficient method to synthesize highly active gold nanoparticles [8, 98].

2.6.2. Chemical reactions catalyzed by supported gold nanoparticles

The potential of supported Au nanoparticles in catalyzing organic reactions is discovered from time to time. Among the earliest and current chemical reactions associated with supported Au nanoparticles as catalysts are presented as follows:

(i) CO oxidation: The CO oxidation reaction at ambient temperature is the earliest discovery of catalysis by Au nanoparticles supported on metal oxides as revealed by Haruta *et al.* [4]. The reaction was conducted in gas phase which yielded CO₂ as the product. For this reaction, Au/TiO₂ is the most extensively studied system [6-8, 99-103]. The combination of Au and titania exhibited amazingly high catalytic activity and was much more active than the other noble metal catalysts at temperatures less than 127 °C [104]. Gold catalytic activity depends on the size of the Au particles as well as the support [8, 74, 90, 101, 103, 105-108]. Goodman and coworkers revealed that the maximum activity was achieved when the Au particles have the diameter of 3.5 nm [100, 109].

(ii) Epoxidation: The Au supported on titania catalyze the selective oxidation of propylene in a gas mixture containing oxygen and hydrogen. This important reaction has attracted many from the chemical industries to explore its potential [110]. Propylene oxide (PO) is one of the important bulk chemicals, which is used to produce polyurethane and polyols. Current industrial processes need two-stages chemical reactions using either Cl₂ or organic peroxides and yield byproducts, stoichiometrically [104]. However with Au catalysts, PO can be produced in one stage (direct epoxidation)

without byproducts other than H₂O. This route is very environmental friendly, and is expected to replace the old processes [111]. This direct epoxidation of propylene significantly depends on the preparation method [112], selection of the support [112], the size of Au particles [110] and the presence of additive [104, 113, 114].

(iii) Water gas-shift reaction: The CO reacts with water vapour to form carbon dioxide and hydrogen in a water-gas shift (WGS) reaction. The WGS is one of the vital industrial reactions owing to its applications in polymer electrolyte fuel cells, automobiles and residential electricity-heat delivery systems. Compared with other metal catalysts such as Ni or Cu, the use of the supported gold catalysts only require a temperature as low as 200 °C. Initially, the activity of Au/TiO₂ in WGS reaction was reported by Sakurai *et al.* [115], followed by Andreeva and co-workers over Au/CeO₂ [116] and Au/CeO₂-Al₂O₃ catalysts [117]. According to the authors, the addition of alumina to the Au/CeO₂ system improved the stability for both gold and ceria dispersion during the catalytic operation.

(iv) Hydrogenation of unsaturated hydrocarbon: The supported Au nanoparticles have been tested for several hydrogenation reaction of hydrocarbon. The earlier works include the hydrogenation of 1,3-butadiene [87]. The total conversion to butenes with 65 - 75 % selectivity to 1-butene was achieved over Au/Al₂O₃, Au/SiO₂, and Au/TiO₂ catalyst by Okumura *et al.* [118]. They also revealed that this reaction was almost structure insensitive in terms of the size of the Au particles (ranged from 2.5 to 5 nm) and the influence of the metal oxide supports.

Later, the selective hydrogenation of α , β -unsaturated aldehydes and ketones to unsaturated alcohol (UA) became the subject of specific interest. The UA production is an important step in industrial synthesis of fine chemicals, particularly in the pharmaceuticals and cosmetic chemicals [83]. Obtaining UA from the hydrogenation of α , β -unsaturated aldehyde and ketone was difficult considering the thermodynamics which favors the hydrogenation of C=C over C=O group [83, 119]. However, gold in the form of nanoparticles is an active redox catalyst for oxygen-containing hydrocarbon, hence was able to reduce alkenes, alkynes, imines and carbonyl at different rates [71, 120-122]. As a result, the selectivity to UA was achieved for acrolein and 2-butenal over Au/ZnO, Au/TiO₂ and Au/ZrO₂ catalysts in a gas phase reaction with Au having a 1 - 5 nm particle size [123-125].

(v) Reduction of nitro group: The selective reduction of a nitro group to amine in the presence of other reducible functionality is a difficult process. It usually requires a stoichiometric amount of reducing agents. Functionalized anilines produced by this particular reaction are industrially important intermediates for pharmaceuticals, fine chemicals and polymers [126]. Therefore, it is desirable to develop chemoselective catalysts for this purpose. Initially, stoichiometric reducing agents such as sodium hydrosulfite, iron, tin and zinc in ammonium hydroxide are used to reduce the aromatic nitro compounds [127]. However these processes are not environmentally sustainable. Moreover iron complexes or doped Raney nickel are also utilized in this reaction, though the drawback lies in its difficulty to be reused. The use of noble metal catalysts such as Pt and Pd can activate the nitro groups as well as carbonyl and double bonds,